

## Supplementary Methods

### **a) Study design**

This study was designed as an investigator-initiated clinical study to investigate the molecular signatures of AD and psoriasis. Procedures were conducted according to the Declaration of Helsinki principles. Informed written consent was obtained from human subjects under a protocol approved by the local ethics board at the University Hospital Schleswig-Holstein, Campus Kiel, Germany (reference: A100/12). Adult patients with a history of AD or psoriasis for at least 3 years attending the dermatology department as well as adult volunteers without personal or familial history of atopic and chronic-inflammatory diseases of German ethnicity were invited to participate. Inclusion criteria for patients were a dermatologist-confirmed diagnosis of active chronic plaque-type psoriasis or AD. Exclusion criteria were presence of any other chronic skin disease, systemic treatment with immune-efficient medication ever, and topical treatment within one week prior to material sampling. AD or psoriasis was diagnosed on the basis of a skin examination by experienced dermatologists according to standard criteria (for AD, the American Academy of Dermatology Consensus Criteria were used) (Boehncke and Schon, 2015, Weidinger and Novak, 2015). From all participants, 9 ml of blood (collected into EDTA) as well as 5mm skin punch biopsies from the upper extremities (under local anesthesia) were obtained. From control individuals, a single biopsy was taken, while pairs of biopsies were taken and from adjacent (at least 50 mm from active lesions) clinically normal (i.e. no signs of erythema, edema, crusting, thickening, scaling or scratch marks) skin in psoriatic or AD patients. Skin tissue specimen were stored in PaxGene tissue containers (PreAnalytiX, Hombrechtikon, Switzerland) at -80°C according to the manufacturer's manual until further processing. A detailed cohort description can be found in **Supplementary Table 1**.

### **b) Filaggrin gene genotyping**

Genomic DNA was isolated from peripheral EDTA blood with the automated chemagic Star workstation protocol (Hamilton Company, Reno, NV) and used to determine the *filaggrin* gene (FLG) status of AD patients and healthy controls. The four most common European mutations R501X, 2282del4, R2447X and S3247X were analyzed with the TaqMan allelic discrimination

method (Applied Biosystems, Carlsbad, CA) following the standard procedures based on the manufacturer's reagents. Probe detection was performed with the Applied Biosystems 7900HT Fast Real-Time PCR System. Results are presented in **Supplementary Table 1**.

***c) Sample processing***

Total RNA was isolated from PAXgene® fixed tissue samples using the AllPrep DNA/RNA Mini Kit (Qiagen, Hilden, Germany) following the manufacturer's specifications. Samples of cases and controls were randomly distributed across the plates and pools before sequencing to minimize batch effects; in total we used 3 runs to obtain RNA-seq data. Preceding RNA isolation all samples were disrupted using innuSPEED Lysis Tubes W (1,4 - 1,6 mm steel beads & 3,5 mm ceramic beads) (Analytik Jena, Jena, Germany) in a SpeedMill Plus (3x 1min intervals) (Analytik Jena) together with 600µl of RLT-Plus-Buffer (Qiagen) including β-Mercaptoethanol and additionally homogenized with QIAshredder spin-columns (Qiagen). In order to assure sufficient concentration, integrity and purity of isolated RNA all samples were measured with the Qubit 2.0 Fluorometer (Qubit RNA HS Assay) (LifeTechnologies, Carlsbad, CA) and the 2200 Tape Station (R6K ScreenTape Assay) (Agilent, Santa Clara, CA) following the manufacturer's instructions. Only samples with a concentration of >50ng/µl, an OD260/280 ≥1.8 and a RNA integrity number (RIN) >7 were included in subsequent library preparation and sequencing.

***d) RNA library preparation and sequencing***

RNA samples were prepared for sequencing using the Illumina Truseq® Stranded total RNA Protocol in combination with the RiboZero rRNA removal Kit, and sequenced on the HiSeq2500 in pools of 10 samples with 2x125bp, producing paired-end reads according to the manufacturer's protocol (Illumina, San Diego, CA). The case and control samples were randomly distributed across the plates and pools before sequencing to minimize batch effects. We sequenced libraries prepared from total RNA extracted from 147 skin biopsies (38 control;

27 psoriasis non-lesional (NL); 28 psoriasis lesional (LL); 27 AD NL; 27 AD LL) donated by 93 individuals.

**e) *RNA-seq data processing***

Low quality reads were filtered from the data using the Illumina CASAVA FASTQ filter. Illumina standard primers were trimmed, and the quality of the data was assessed using FastQC (vs 0.11.3) (Andrews, 2010). Paired reads were mapped to the human reference genome (b37) using STAR (Dobin et al., 2013), only uniquely mapped read pairs were retained. Number of reads for each gene was counted using HTSeq (Anders et al., 2015), only genes with on average  $\geq 1$  read/sample were used in our analysis. TMM was used to normalize the RNA-seq data (Robinson and Oshlack, 2010), and we applied voom transformation to model the mean-variance relationship of the expression data (Law C. W. et al., 2014).

**f) *Statistical and bioinformatics analysis***

We conducted differential expression analysis between different conditions using empirical Bayes linear model as implemented in the limma package (Ritchie et al., 2015), controlling for individual specific effect (for nonlesional vs. lesional skin comparison) and gender effect (for normal vs. nonlesional/lesional skin comparison); False discovery rate (FDR)  $\leq 5\%$  and  $|\log_2$  Fold Change (FC)|  $\geq 1$  were used to declare significance. Functional enrichment analysis was performed using the hypergeometric test for pathways/functions compiled from Gene Ontology (Ashburner et al., 2000), KEGG (Kanehisa et al., 2012), and Biocarta (Nishimura, 2001), and only those with  $\geq 10$  and  $\leq 300$  annotated genes were examined;  $FDR \leq 10\%$  and Observed/Expected ratio  $\geq 2$  were declared significant. By using the current criteria (i.e.  $FDR \leq 5\%$  and with more than 2 fold change between two groups) and assuming  $>10\%$  of genes truly differentially expressed (with on average  $>500$  read counts/sample, estimated from our cohort)

from the 31,364 genes we examined, retrospective power calculation estimates >75% of statistical power (Guo et al., 2014).

For illustration purposes, we grouped similar functions and presented the groupings in a piechart using ClueGO (Bindea et al., 2009). To identify genes that are close to T-cell specific chromatin marks, we first retrieved T-cell H3K27ac peak signals from a previous study (Farh et al., 2015), and, for each cell type, we computed the cell-type specific ratio of each peak's by comparing the signal in the cell type with the average of the remaining cell types. The 10,000 peaks with the highest ratios for each cell type were screened for cell-specific genes within a 5k bp interval. We performed the classification task (e.g. psoriatic vs AD lesional skin) using the Random Forest classifier in the MLR package (Bischi et al., 2016), and the top features were selected according to backward selection with permutation importance; the final Area under Receiver Operating Characteristic (AUROC) was estimated (using the selected features) from three-fold cross validation with 100-repetitions.

We compiled the expert-curated chemical/drug -- gene interactions from the Comparative Toxicogenomics Database (CTD) (Davis et al., 2016), DrugBank (Law V. et al., 2014) and PharmGKB (Hewett et al., 2002), and the chemical/drug -- disease associations from CTD and National Drug File-Reference Terminology (NDF-RT) (Carter et al., 2002). Although these resources also include chemicals, we apply a lexicon to only include associations/interactions involving three types of drugs (antibiotics, clinical drugs and pharmacologic active substances). All the resources use customized identifiers for drugs and diseases, thus recognizing duplicates across the resources is challenging. We therefore replaced the drug identifiers with customized identifiers from our previous work (Raja et al., 2017), plus the diseases' concept identifier (CUI) from UMLS Metathesaurus.

### ***g) Cytokine stimulation in keratinocytes***

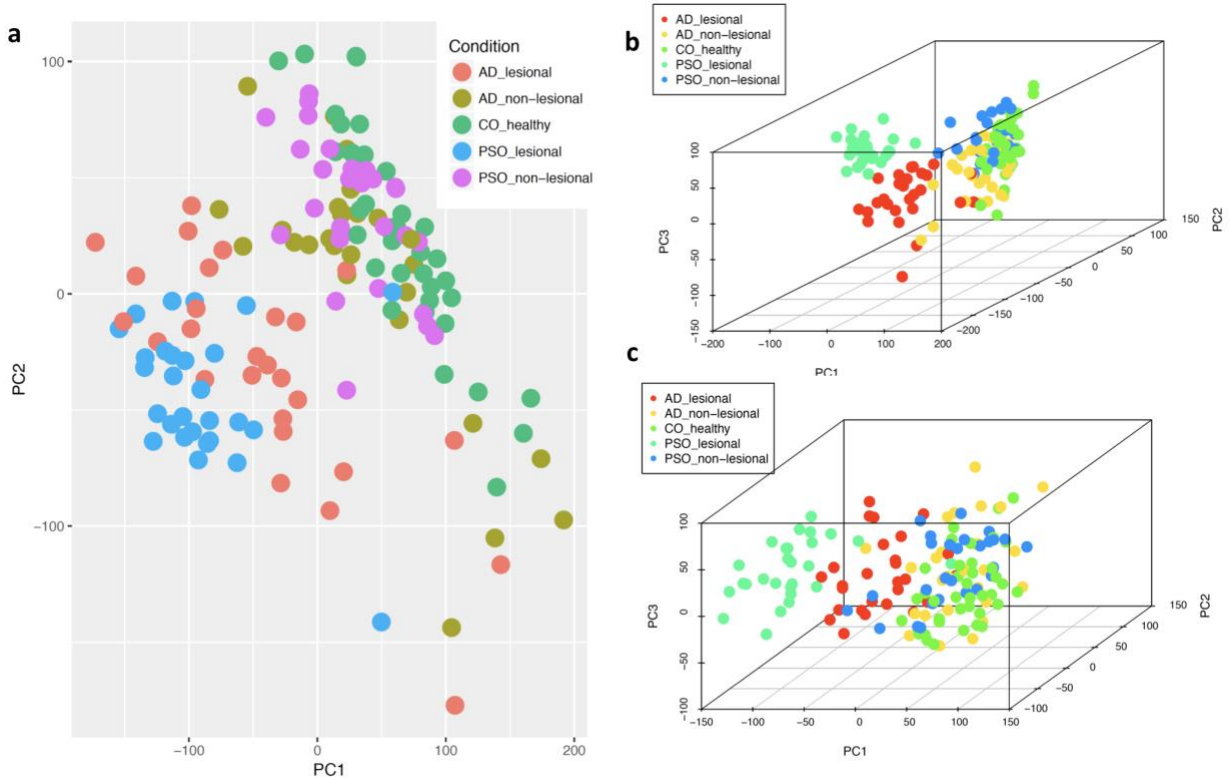
We determined whether the DEGs identified in our experiments were regulated by stimulations with various cytokines in keratinocytes. We obtained 50 normal human keratinocytes from 50 different healthy adults. Keratinocytes were grown in 12 well plate in 154 CF medium (Thermo Fisher #M154CF500) with human keratinocyte growth supplement (Thermo Fisher #S0015). Keratinocytes were grown to confluency at which time the complete medium (with supplements) was replaced by basal 154 CF medium (without supplements). Cells were then stimulated with cytokines (IL-4, IL-13, IFN- $\alpha$ , IFN- $\gamma$ , TNF- $\alpha$ , IL-17A, IL-36 $\alpha$ , IL-36 $\beta$ , IL-36 $\gamma$ , R&D Systems) individually at 10 ng/ml concentration. After 8 hrs cells were harvested and RNA was isolated using RNeasy Plus Mini kit (Qiagen # 74136). RNA was analyzed by RNA Nano Chips (Agilent Technologies) and sequenced (Sarkar et al., 2018).

### ***h) Immunohistology***

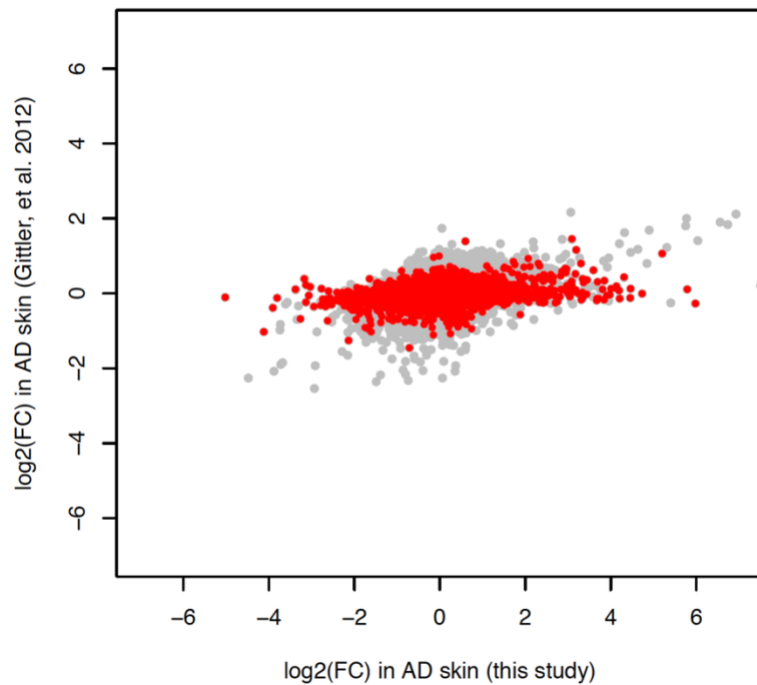
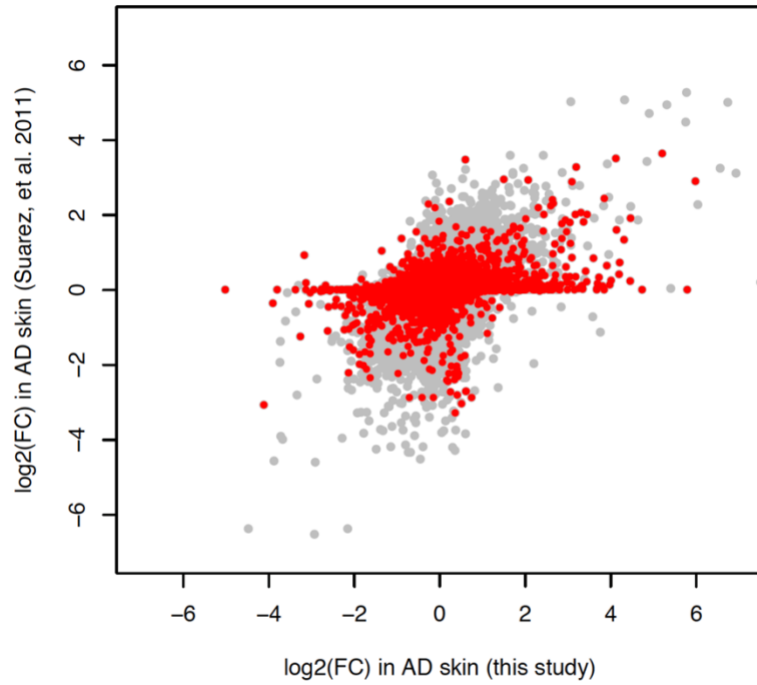
Sections were taken from formalin-fixed, paraffin-embedded biopsies. Tissue slides underwent thorough manual quality control check for the following parameters: dermis and epidermis present on the slide, tissue is well aligned on the glass without loss of large parts of the biopsy material, staining intensity is visible and present in the expected cell component. If any of the criteria were not met, reevaluation on freshly cut material from the identical biopsy was performed. If the second evaluation did not show concordance with the criteria, the slide was excluded from further processing for the digital image analysis. Tissue slides, stained with CD8, were digitally scanned at x20 magnification using a Hamamatsu Nanozoomer in brightfield mode. Quantitative image analysis was performed by on whole slide scanned images using Definiens Tissue Studio® software. A customized algorithm was developed per marker in Tissue Studio® using a subset of the study images. The customized algorithm was developed to accurately detect the whole tissue or if required, segment the specified regions of interest (ROI)

within the whole tissue section. Cellular analysis thresholds were then optimized per algorithm to specifically detect positive cells for the immunohistochemistry markers within the tissue ROI. The algorithms were then applied objectively to each section to quantify the required parameters. Evaluation was performed for total cell count (sum of epidermal and dermal cell counts) on the CD8 stains. The analyzed area was measured in mm<sup>2</sup> and based on the absolute cell counts calculation of cells per mm<sup>2</sup> was performed.

## Supplementary Figures

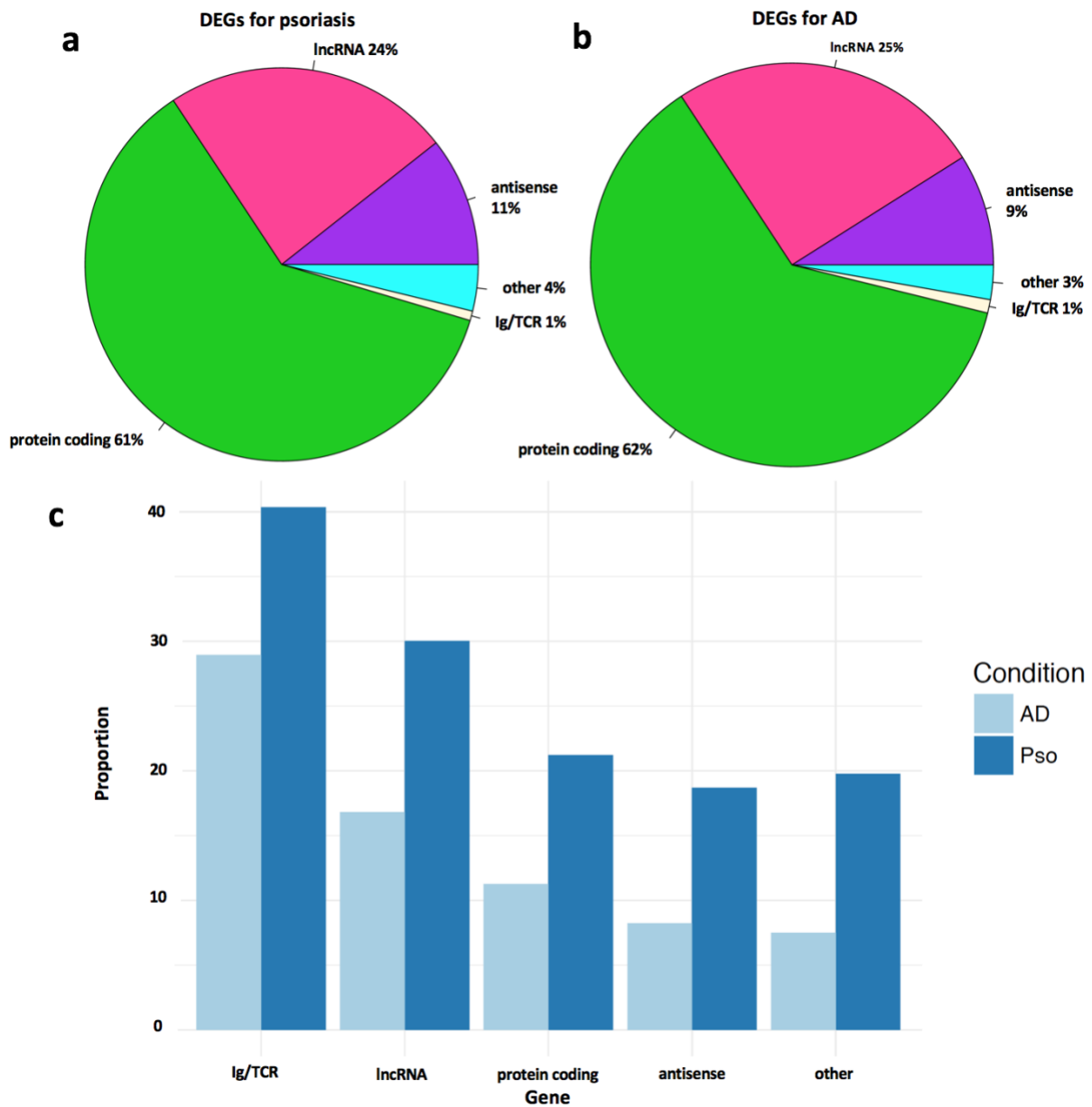


**Supplementary Figure 1.** a) top two principal components computed using the transcriptomes of the samples; b) the top three principal components using the transcriptome of the samples; c) the top three principal components after adjusting the batch variable estimated by the SVA algorithm.

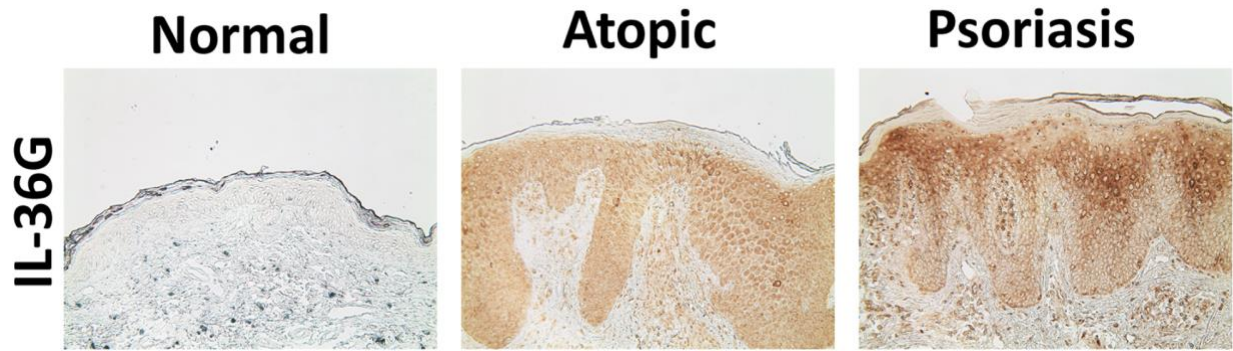


**Supplementary Figure 2. Comparing the magnitude of dysregulation (Fold Change in logarithmic scale) in AD skin measured in this study (x-axis) versus previous microarray studies. Each point represents a gene that is common in both platforms; red color represents genes expressing in the lower 25% of the transcriptome.**

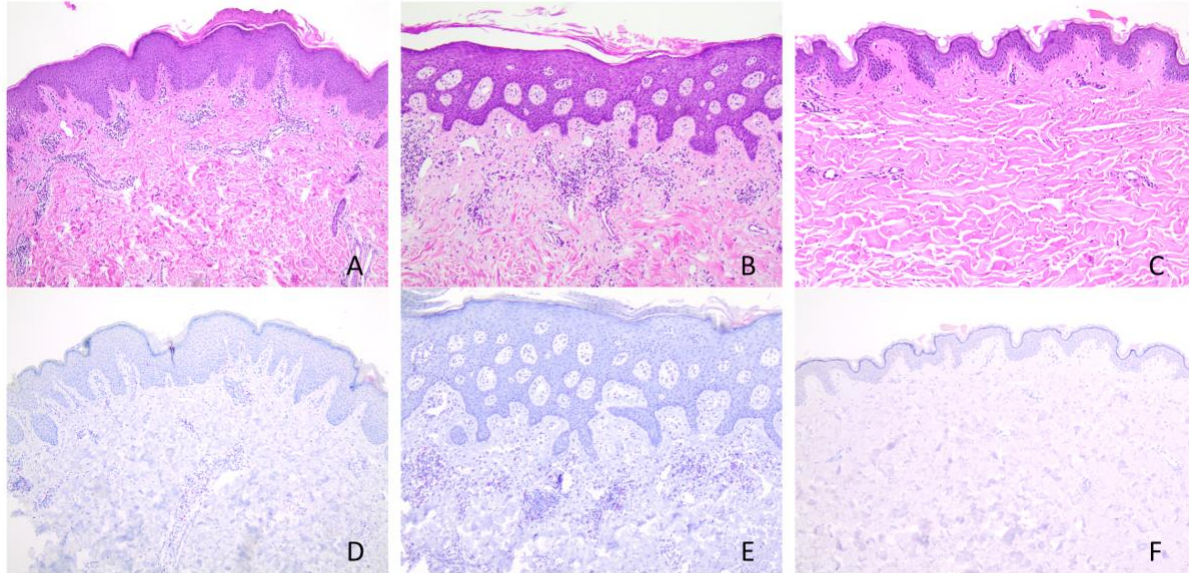




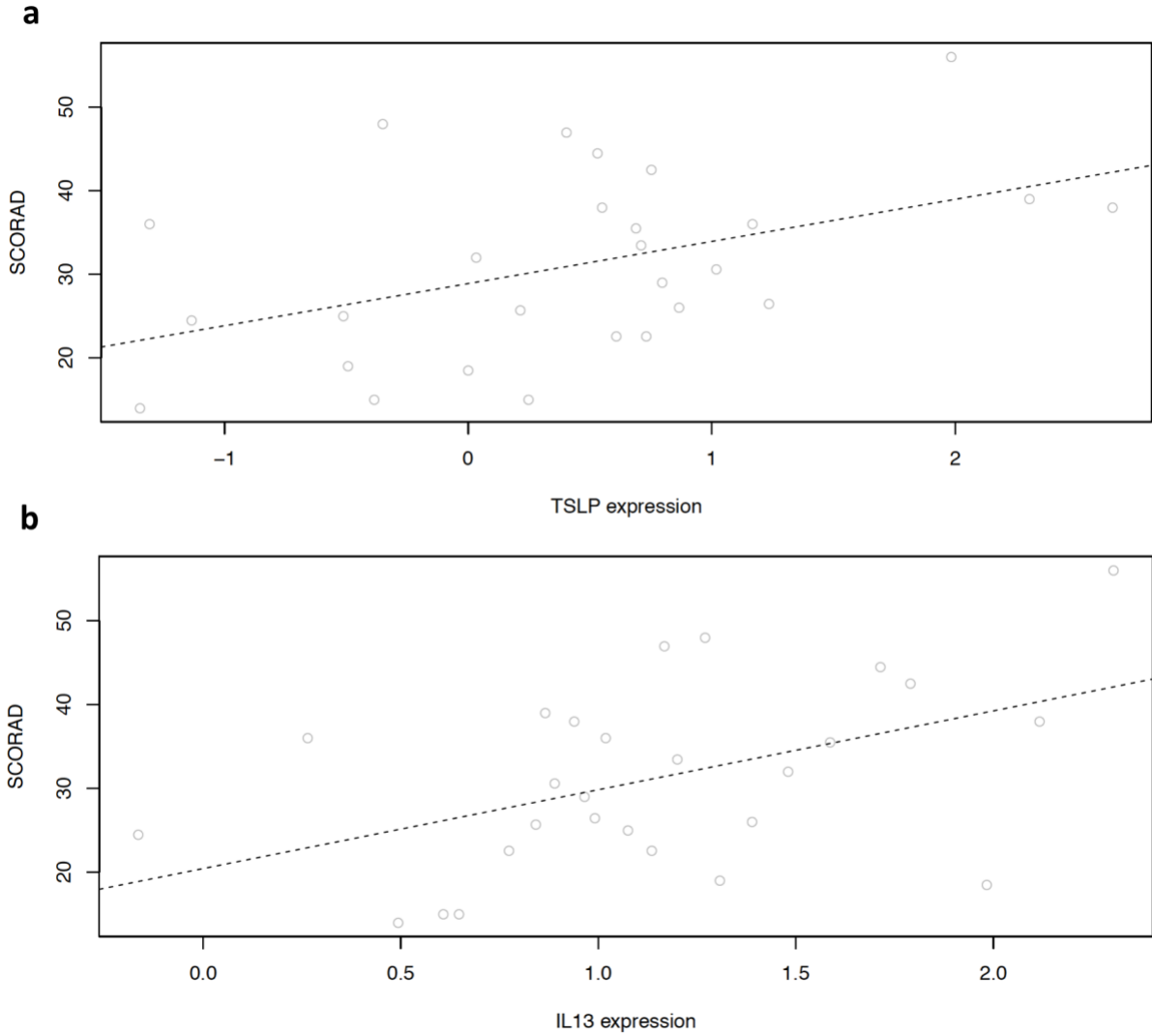
**Supplementary Figure 3. The proportion of different gene categories in the DEGs for psoriasis (a) and atopic dermatitis (b). (c). For each category, the proportion of DEGs.**



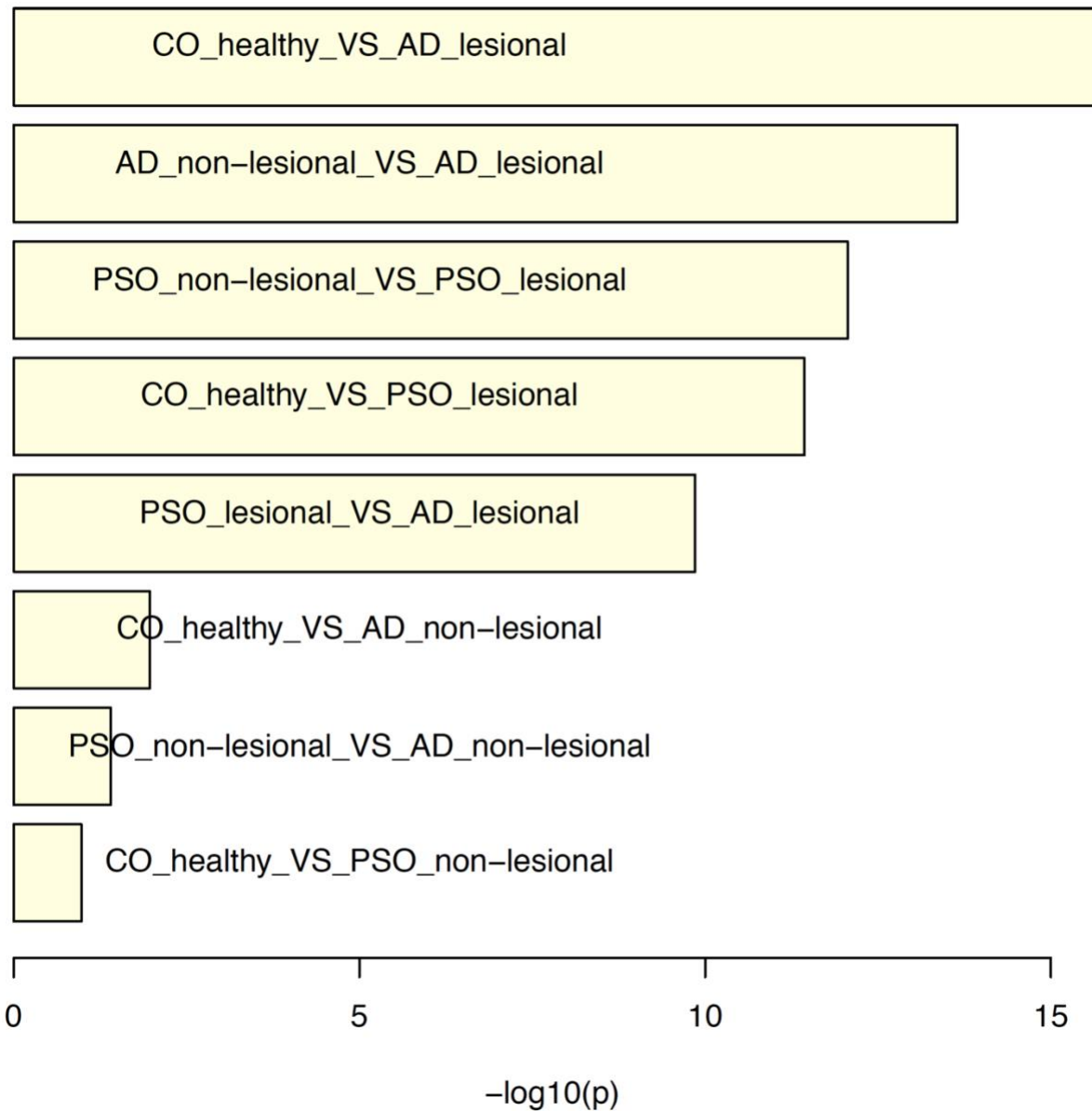
**Supplementary Figure 4. Immunohistochemistry illustrates the detection of IL-36G in the skin of atopic dermatitis and psoriasis, concordant with the expression data.**



**Supplementary Figure 5. Lesional AD skin (A) with acanthotic thickening of the epidermis and parakeratosis. Perivascular infiltration of lymphomononuclear cells mainly in the dermis and focal epidermotropic lymphocytes. The lesional psoriatic skin (B) shows an acanthotic epidermis with parakeratosis and hypogranulosis and perivascular lymphomononuclear infiltrates in the upper dermis. The healthy control skin (C) displays a thin epidermis with regular structure and scarce perivascular lymphomononuclear infiltrates. CD8 is expressed in lymphocytic cells in the dermal compartment in lesional AD (D), lesional psoriasis (E) and control skin (F), accounting approximately for a quarter of all lymphocytes in each sample. In relation to the amount of lymphocytic infiltrates, the absolute count of CD8 positive cells is higher in D and E. Original magnification x100 in A-F.**



**Supplementary Figure 6. Correlation between SCORAD with normalized expression of TSLP (a) and IL13 (b) of AD lesional skin samples**



**Supplementary Figure 7. The enrichment analysis for AD drug targets among the genes dysregulated in different differential expression analysis.**

## Supplementary Tables

**Supplementary Table 1. Cohort description:** Continuous traits as mean and standard deviation for atopic dermatitis patients (AD), psoriasis patients (Pso) and healthy control individuals (Healthy). Filaggrin (FLG) status (R501X, 2282del4, R2447X, S3247X) determined in AD and healthy control individuals only.

	AD	Pso	Healthy
Number of individuals (male/female)	27 (17/10)	28 (14/14)	38 (16/22)
Age	34.07+/-10.96	41.89+/-15.74	32.63+/-11.64
Objective Scord / PASI	31.11+/-10.96	9.54+/-3.49	-
BMI	25.07+/-5.1	28.65+/-5.69	24.16+/-4.22
Age onset <6	80.77	7.14	-
FLG mutation carriers N (%)	7 (25.93)	NA	1 (2.63)
Asthma/Rhinitis (%)	48.15/62.96	-/-	0/0
Dennie-Morgan lines: weak/moderate/strong (%)	37.04/11.11/0	-/-/-	0/0/0
Herthoge's sign: weak/moderate/strong (%)	14.81/0/0	5.26/0/0	-/-/-
Palmar hyperlinearity: weak/moderate/strong (%)	37.04 /22.22/3.7	-/-/-	5.26/0/0
Sebostasis weak/moderate/strong (%)	29.63/44.44/22.22	-/-/-	2.63/0/0
Keratosis pilaris weak/moderate/strong	37.04/11.11/0	-/-/-	7.89/5.26/0
PsA: questionable/yes (%)	-/-	28.57/14.29	-/-

**Supplementary Table 2. Sample description. Clinical and molecular features collected for each samples used in the RNA-seq analysis.**

ID.pheno	Trait	Sex	Age	FLG Mutation	Severity (ScorAD/PASI)	Rhinitis	Asthma	PsA	biopsy site non-lesional	biopsy site lesional	Dennie	Hertoghe	Palmar hyperlinearity	Xerosis	Keratosis pilaris
AD_004	AD	female	48	no	35.5	yes	yes		upper arm flexural right	upper arm flexural left	moderate	no	weak	moderate	no
AD_005	AD	male	43	no	44.5	yes	yes		upper arm flexural left	upper arm flexural right	no	no	moderate	moderate	weak
AD_006	AD	male	25	2282del4	25	no	no		upper arm flexural left	upper arm flexural right	weak	weak	moderate	moderate	weak
AD_007	AD	male	33	R244X	15	yes	no		upper arm flexural left	antecubital fossa left	no	no	moderate	weak	weak
AD_009	AD	male	45	2282del4	32	yes	yes		upper arm flexural left	antecubital fossa left	no	no	moderate	moderate	weak
AD_011	AD	male	45	no	36	yes	yes		upper arm flexural left	upper arm flexural left	no	no	weak	weak	moderate
AD_014	AD	male	37	no	48	yes	no		upper arm flexural left	upper arm flexural left	no	no	weak	moderate	no
AD_016	AD	female	25	no	18.5	no	no		upper arm flexural left	upper arm flexural left	no	no	weak	moderate	moderate
AD_017	AD	female	42	no	38	yes	yes		upper arm flexural left	upper arm flexural left	weak	no	moderate	strong	weak
AD_019	AD	female	22	no	24.5	no	no		upper arm flexural left	antecubital fossa left	no	no	no	moderate	weak
AD_020	AD	female	43	no	42.5	yes	yes		upper arm flexural right	antecubital fossa	weak	no	weak	strong	weak
AD_021	AD	female	29	no	15	no	no		upper arm flexural left	antecubital fossa left	weak	no	no	weak	no
AD_023	AD	male	47	R244X/2282del4	47	yes	yes		upper arm flexural left	upper arm flexural left	weak	weak	strong	strong	weak
AD_024	AD	female	45	no	22.6	no	yes		upper arm flexural right	upper arm flexural right	no	no	weak	strong	weak
AD_025	AD	female	22	no	22.6	no	no		upper arm flexural left	antecubital fossa left	weak	no	no	moderate	no
AD_026	AD	male	19	no	33.5	yes	yes		upper arm flexural left	antecubital fossa left	no	no	weak	weak	no
AD_027	AD	female	22	no	14	yes	yes		upper arm flexural left	upper upper arm flexural left	no	weak	no	moderate	no
AD_028	AD	male	31	no	19	yes	yes		upper arm flexural right	upper arm flexural right	weak	no	weak	moderate	no
AD_029	AD	male	21	no	25.7	yes	no		upper arm flexural left	upper arm flexural left	moderate	no	weak	no	no
AD_030	AD	female	23	no	26.5	no	no		upper arm flexural right	antecubital fossa right	no	no	no	weak	no
AD_031	AD	male	24	no	30.6	no	no		upper arm flexural left	upper arm flexural left	weak	no	no	moderate	moderate
AD_032	AD	male	53	2282del4	29	no	no		upper arm flexural left	antecubital fossa right	no	no	moderate	moderate	weak
AD_033	AD	male	48	no	39	yes	yes		upper leg flexural right	upper leg flexural right	moderate	no	no	strong	no
AD_034	AD	male	30	R501X	38	yes	yes		upper arm flexural right	upper arm flexural right	no	no	moderate	moderate	no
AD_035	AD	male	19	no	26	yes	no		upper arm flexural left	lower arm left	weak	no	no	weak	no
AD_036	AD	male	45	R501X/2282del4	56	yes	no		upper arm flexural left	upper arm flexural left	no	no	moderate	strong	no
AD_037	AD	male	34	no	36	no	no		upper arm flexural left	upper arm flexural left	weak	weak	no	weak	no
PSO_001	PSO	female	28		3.3			yes	upper arm extensor left	elbow left					
PSO_002	PSO	male	50		5			no	upper arm flexural left	upper arm flexural left					
PSO_003	PSO	female	50		6.2			yes	upper leg flexural left	upper leg flexural left					
PSO_005	PSO	female	33		4.3			no	lower leg flexural right	lower leg flexural right					

ID.pheno	Trait	Sex	Age	FLG Mutation	Severity (ScorAD/P ASI)	Rhinitis	Asthma	PsA	biopsy site non-lesional	biopsy site lesional	Dennie	Hertoghe	Palmar hyperlinearity	Xerosis	Keratosis pilaris
PSO_006	PSO	female	50		7			no	lower leg flexural left	lower leg flexural left					
PSO_007	PSO	female	68		3.8			unknown	upper arm extensor right	upper arm extensor right					
PSO_008	PSO	female	35		5			no	upper arm flexural left	elbow left					
PSO_009	PSO	male	71		6.2			yes	lower leg flexural left	lower arm flexural left					
PSO_011	PSO	male	53		8.3			yes	lower leg extensor left	lower leg extensor left					
PSO_012	PSO	female	46		5.8			unknown	lower leg extensor left	lower leg extensor left					
PSO_014	PSO	male	22		6.8			no	upper arm extensor left	upper arm extensor left					
PSO_015	PSO	male	49		22.4			unknown	upper arm extensor left	upper arm extensor left					
PSO_016	PSO	male	23		5.4			no	upper arm extensor left	upper arm extensor left					
PSO_017	PSO	male	30		6.6			no	lower arm extensor left	lower arm extensor left					
PSO_018	PSO	female	38		1.8			no	upper arm extensor left	upper arm extensor left					
PSO_020	PSO	female	21		2.7			unknown	upper leg flexural left	upper leg flexural left					
PSO_023	PSO	female	36		1.2			unknown	upper arm extensor left	elbow left					
PSO_024	PSO	male	69		2.9			no	upper arm extensor right	elbow right					
PSO_027	PSO	male	46		3.6			no	upper arm flexural left	elbow left					
PSO_028	PSO	male	41		9.7			no	upper arm extensor left	upper arm extensor left					
PSO_029	PSO	female	70		2			unknown	upper arm extensor right	elbow right					
PSO_030	PSO	male	52		6.8			no	upper arm extensor right	elbow right					
PSO_031	PSO	male	40		11.4			no	upper arm extensor right	elbow right					
PSO_033	PSO	female	28		4.5			no	upper arm extensor right	upper arm extensor right					
PSO_034	PSO	male	28		4			unknown	upper arm flexural left	upper arm flexural left					
PSO_035	PSO	male	24		1.3			no	upper arm flexural left	upper arm flexural left					
PSO_036	PSO	female	18		3.5			no	upper arm extensor left	upper arm extensor left					
PSO_037	PSO	female	54		10.5			unknown	upper arm extensor right	upper arm extensor right					
CTRL_002	CTRL	female	42	no					upper arm flexural left		no	no	no	no	no
CTRL_003	CTRL	female	25	no					upper arm flexural left		no	no	no	no	no
CTRL_004	CTRL	female	28	no					upper arm flexural left		no	no	no	no	no
CTRL_006	CTRL	female	24	no					upper arm flexural left		no	no	no	no	no
CTRL_008	CTRL	male	28	no					upper arm flexural right		no	no	no	no	weak
CTRL_009	CTRL	female	33	no					upper arm flexural left		no	no	no	no	weak
CTRL_010	CTRL	female	27	no					upper arm flexural left		no	no	no	no	no
CTRL_011	CTRL	male	26	no					upper arm flexural left		no	no	no	no	moderate
CTRL_013	CTRL	male	42	no					upper arm extensor right		no	no	no	no	no



ID.pheno	Trait	Sex	Age	FLG Mutation	Severity (ScorAD/PAS I)	Rhinitis	Asthma	PsA	biopsy site non-lesional	biopsy site lesional	Dennie	Hertoghe	Palmar hyperlinearity	Xerosis	Keratosis pilaris
CTRL_014	CTRL	male	24	no		no	no		upper arm flexural left		no	no	no	no	no
CTRL_015	CTRL	female	28	no		no	no		upper arm flexural left		no	no	no	no	no
CTRL_016	CTRL	female	32	no		no	no		upper arm flexural left		no	no	no	no	no
CTRL_017	CTRL	male	30	no		no	no		upper arm flexural left		no	no	no	no	no
CTRL_018	CTRL	male	23	no		no	no		upper arm flexural left		no	no	no	no	no
CTRL_019	CTRL	female	40	no		no	no		upper arm extensor left		no	no	weak	no	moderate
CTRL_020	CTRL	male	26	no		no	no		upper arm flexural left		no	no	no	weak	no
CTRL_022	CTRL	male	47	no		no	no		upper arm flexural left		no	no	no	no	no
CTRL_024	CTRL	female	47	no		no	no		upper arm flexural left		no	no	no	no	no
CTRL_025	CTRL	female	25	no		no	no		upper arm flexural left		no	weak	no	no	no
CTRL_026	CTRL	female	31	no		no	no		upper arm flexural left		no	weak	no	no	no
CTRL_029	CTRL	male	40	no		no	no		upper arm flexural left		no	no	no	no	no
CTRL_030	CTRL	male	40	no		no	no		upper arm flexural left		no	no	no	no	no
CTRL_031	CTRL	male	54	no		no	no		upper arm flexural left		no	no	no	no	no
CTRL_032	CTRL	male	37	no		no	no		upper arm flexural right		no	no	no	no	no
CTRL_033	CTRL	female	52	no		no	no		upper arm extensor left		no	no	no	no	no
CTRL_034	CTRL	male	61	no		no	no		upper arm flexural left		no	no	no	no	no
CTRL_035	CTRL	female	29	no		no	no		upper arm flexural left		no	no	no	no	no
CTRL_036	CTRL	female	25	no		no	no		upper arm flexural left		no	no	no	no	no
CTRL_037	CTRL	male	22	no		no	no		upper arm flexural left		no	no	no	no	weak
CTRL_038	CTRL	female	20	no		no	no		upper arm flexural left		no	no	no	no	no
CTRL_039	CTRL	female	19	no		no	no		upper arm extensor left		no	no	weak	no	no
CTRL_040	CTRL	female	20	no		no	no		upper arm flexural left		no	no	no	no	no
CTRL_041	CTRL	female	57	no		no	no		upper arm extensor right		no	no	no	no	no
CTRL_042	CTRL	female	20	2282del4		no	no		upper arm flexural left		no	no	no	no	no
CTRL_043	CTRL	female	24	no		no	no		upper arm flexural left		no	no	no	no	no
CTRL_044	CTRL	male	18	no		no	no		upper arm flexural right		no	no	no	no	no
CTRL_045	CTRL	female	25	no		no	no		upper arm flexural right		no	no	no	no	no
CTRL_046	CTRL	male	49	no		no	no		upper arm flexural left		no	no	no	no	no

**Supplementary Table 3. Transcriptomic studies conducted for AD/Eczema.** Only show the number of samples that have been profiled for transcriptome, remained after quality control, and presented in the paper (if the number cannot be determined in the paper, the number of samples deposited in the corresponding GEO was used). ^same control individuals; \*same patients; #the study used skin tape strip for profiling the transcriptome.

Study	Platform	Study treatment response	Control	Pso uninvolved	Pso lesional	AD/Eczema uninvolved	AD/Eczema lesional
Nomura I, et al. 2003. <i>JACI</i>	Microarray	NA	NA	NA	6	NA	7
Guttman-Yassky E et al. 2009. <i>JACI</i>	Microarray	NA	9^	NA	15	NA	9
Suarez-Farinas Mayte, et al. 2011. <i>JACI</i>	Microarray	NA	8	NA	NA	12	13
Tintle S, et al. 2011. <i>JACI</i>	Microarray	UVB phototherapy	NA	NA	NA	12	12
Choy DF et al. 2012. <i>JACI</i>	Microarray	NA	5	NA	14	NA	12
Gittler JK et al. 2012. <i>JACI</i>	Microarray	NA	15^	NA	NA	8	8 chronic/8 acute
Cole C et al. 2014. <i>JACI</i>	<b>RNA-Seq</b>	NA	10	NA	NA	26	NA
Quaranta M et al. 2014. <i>Sci Trans Med</i>	Microarray	NA	NA	NA	24 psoriatic patients also with eczema	NA	24 eczema patients also with psoriasis
Rodriguez E, et al. 2014. <i>JID</i>	Microarray	NA	14 epidermal	NA	NA	7 epidermal	12 epidermal
Khattari S, et al. 2014. <i>JACI</i>	Microarray	Cyclosporine	NA	NA	NA	19*	19*
Beck LA, et al. 2014. <i>NEJM</i>	microarray	dupilumab	NA	NA	NA	7	16
Suarez-Farinas M, et al. 2015. <i>JACI</i>	<b>Microarray &amp; RNA-seq</b>	NA	NA	NA	NA	18*	18*
Brunner, PM, et al. 2016. <i>JACI</i>	Microarray	Topical glucocorticosteroids	NA	NA	NA	9	14
Malik K. et al. 2017. <i>Clin Exp Allergy</i>	Microarray	House dust mite atopy patch test	14	NA	NA	8	8
Dyjack N, et al. 2018. <i>JACI</i> <sup>#</sup>	RNA-seq	NA	13	NA	NA	18	12
<b>This study</b>	<b>RNA-seq</b>	NA	38	27	28	27	27

**Supplementary Table 4. Number of differentially expressed genes in each of the comparisons.**

DE analysis	Number of Genes		
	DEGs	Up-regulated	Down-regulated
Healthy vs Pso non-lesional	246	82	164
Healthy vs Pso lesional	6763	2502	4261
Pso non-lesional vs Pso lesional	5156	2232	2924
Healthy vs AD non-lesional	180	98	82
Healthy vs AD lesional	3450	1529	1921
AD non-lesional vs AD lesional	1785	919	866
Pso non-lesional vs AD non-lesional	185	117	68
Pso lesional vs AD lesional	2030	1259	771

**Supplementary Table 5. Functional enrichment results for lesional DEGs In Excel Table**

**Supplementary Table 6. Functional enrichment results for uninvolved DEGs In Excel Table**

**Supplementary Table 7. Read counts obtained for IL4 and IL13 for all samples**

**Supplementary Table 8. Cell type enrichment analysis for different differential expression analysis**

**Supplementary Table 9. Proportion of CD8 cells obtained from the quantitative immunochemistry results.**

**Supplementary Table 10. Table for top features in classification.**

	Ranking of selected features	Selected features
<b>Normal vs uninvolved</b>		
<b>AD</b>	1	<i>IL13</i>
	2	<i>EBI3</i>
	3	<i>IL26</i>
	4	<i>IL20</i>
	5	<i>IL5</i>
	6	<i>IL36A</i>
	7	<i>IL36G</i>
<b>Normal vs uninvolved</b>		
<b>Pso</b>	1	<i>IL36G</i>
	2	<i>IL19</i>
	3	<i>IL18</i>
	4	<i>IL36A</i>
	5	<i>EBI3</i>
	6	<i>IL13</i>

**Supplementary Table 11. Spearman correlation and significance level between gene expression and severity score in psoriatic lesional (PASI) and AD lesional (SCORAD) skin.**

**Supplementary Table 12. Current AD drugs (from the drug databases used in this study) whose targets are differentially expressed in AD lesioanl skin.**

## References

- Anders S, Pyl PT, Huber W. HTSeq--a Python framework to work with high-throughput sequencing data. *Bioinformatics* 2015;31(2):166-9.
- Andrews S. FastQC: a quality control tool for high throughput sequence data., <http://www.bioinformatics.babraham.ac.uk/projects/fastqc>; 2010 [accessed].
- Ashburner M, Ball CA, Blake JA, Botstein D, Butler H, Cherry JM, et al. Gene ontology: tool for the unification of biology. The Gene Ontology Consortium. *Nature genetics* 2000;25(1):25-9.
- Bindea G, Mlecnik B, Hackl H, Charoentong P, Tosolini M, Kirilovsky A, et al. ClueGO: a Cytoscape plug-in to decipher functionally grouped gene ontology and pathway annotation networks. *Bioinformatics* 2009;25(8):1091-3.
- Bischl B, Lang M, Kotthoff L, Schiffner J, Richter J, Studerus E, et al. mlr: Machine Learning in R. *Journal of Machine Learning Research* 2016;17(170):1-5.
- Boehncke WH, Schon MP. Psoriasis. *Lancet* 2015;386(9997):983-94.
- Carter JS, Brown SH, Erlbaum MS, Gregg W, Elkin PL, Speroff T, et al. Initializing the VA medication reference terminology using UMLS metathesaurus co-occurrences. *Proc AMIA Symp* 2002:116-20.
- Davis AP, Grondin CJ, Johnson RJ, Sciaky D, King BL, McMorran R, et al. The Comparative Toxicogenomics Database: update 2017. *Nucleic Acids Res* 2016.
- Dobin A, Davis CA, Schlesinger F, Drenkow J, Zaleski C, Jha S, et al. STAR: ultrafast universal RNA-seq aligner. *Bioinformatics* 2013;29(1):15-21.
- Farh KK, Marson A, Zhu J, Kleinewietfeld M, Housley WJ, Beik S, et al. Genetic and epigenetic fine mapping of causal autoimmune disease variants. *Nature* 2015;518(7539):337-43.
- Guo Y, Zhao S, Li CI, Sheng Q, Shyr Y. RNAseqPS: A Web Tool for Estimating Sample Size and Power for RNAseq Experiment. *Cancer Inform* 2014;13(Suppl 6):1-5.
- Hewett M, Oliver DE, Rubin DL, Easton KL, Stuart JM, Altman RB, et al. PharmGKB: the Pharmacogenetics Knowledge Base. *Nucleic Acids Res* 2002;30(1):163-5.
- Kanehisa M, Goto S, Sato Y, Furumichi M, Tanabe M. KEGG for integration and interpretation of large-scale molecular data sets. *Nucleic Acids Res* 2012;40(Database issue):D109-14.
- Law CW, Chen Y, Shi W, Smyth GK. voom: Precision weights unlock linear model analysis tools for RNA-seq read counts. *Genome Biol* 2014;15(2):R29.
- Law V, Knox C, Djoumbou Y, Jewison T, Guo AC, Liu Y, et al. DrugBank 4.0: shedding new light on drug metabolism. *Nucleic Acids Res* 2014;42(Database issue):D1091-7.
- Nishimura D. Biocarta. *Biotech Software & Internet Report* 2001;2(3):117-20.
- Raja K, Patrick M, Elder JT, Tsoi LC. Machine learning workflow to enhance predictions of Adverse Drug Reactions (ADRs) through drug-gene interactions: application to drugs for cutaneous diseases. *Sci Rep* 2017;7(1):3690.
- Ritchie ME, Phipson B, Wu D, Hu Y, Law CW, Shi W, et al. limma powers differential expression analyses for RNA-sequencing and microarray studies. *Nucleic Acids Res* 2015;43(7):e47.
- Robinson MD, Oshlack A. A scaling normalization method for differential expression analysis of RNA-seq data. *Genome Biol* 2010;11(3):R25.

Sarkar MK, Hile GA, Tsoi LC, Xing X, Liu J, Liang Y, et al. Photosensitivity and type I IFN responses in cutaneous lupus are driven by epidermal-derived interferon kappa. *Ann Rheum Dis* 2018.

Weidinger S, Novak N. Atopic dermatitis. *Lancet* 2015.



